JOC*Article*

Properties of a Triazolopyridine System as a Molecular Chemosensor for Metal Ions, Anions, and Amino Acids†

Mimoun Chadlaoui, Belén Abarca,* Rafael Ballesteros, and Carmen Ramírez de Arellano

Departament de Química Orgánica, Facultat de Farmacia, Universitat de València, 46100 Burjassot, Spain

Juan Aguilar, Ricardo Aucejo, and Enrique García-España*

Departament de Química Inorgánica, ICMOL, Universitat de València, Edificio de Institutos, Apdo Correos 22085, 46071 Valencia, Spain

enrique.garcia-es@uv.es; belen.abarca@uv.es

Received June 27, 2006

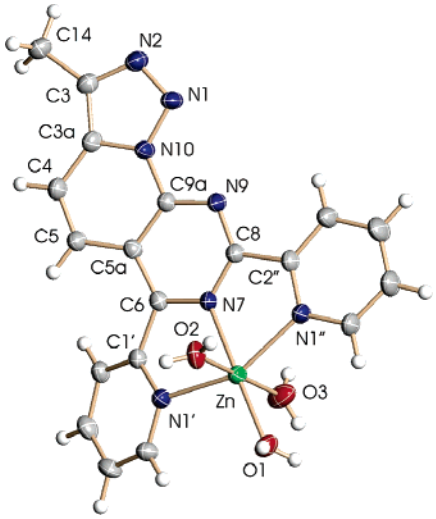

The characteristics as a chemosensor of the compound 3-methyl-6,8-di(2-pyridyl)-[1,2,3]triazolo[5′,1′:6,1]pyrido[2,3-*d*]pyrimidine (**1**) have been analyzed. Interaction with Cu^{2+} produces a quenching of the fluorescence, while interaction with Zn^{2+} leads to a quenching of the fluorescence followed by a bathochromic shift. The crystal structure of the $[Zn(\mathbf{1})(H_2O)_3](ClO_4)_2]\cdot H_2O$ complex shows the coordination of Zn^{2+} through the terpyridine moiety. The octahedral site is completed by three water molecules. Interactions of the Zn^{2+} complex with the anions sulfate, nitrate, nitrite, and dihydrogenphosphate in ethanol produce hypsochromic shifts and restoration of the fluorescence whose magnitude depends on the anion involved. The maximum interaction is observed for $H_2PO_4^-$. Interactions of the Zn^{2+} complex with the amino acids L-aspartate and L-glutamate have also been explored showing a higher interaction with L-aspartate.

Introduction

Molecules having extended conjugate aromatic systems with electron-donating and electron-withdrawing groups can undergo intramolecular charge-transfer processes upon light excitation. Metal ion or proton coordination to the donor or acceptor groups changes the efficiency of the intramolecular charge transfer. Cation coordination to the electron-donating group decreases its electron-donating ability and will reduce the conjugation leading to a blue shift in the absorption spectrum and to a decrease in the molar absorption coefficient.[1] Conversely, coordination of the cation to the electron-accepting group yields

† Dedicated to Prof. Dr. José Elguero Bertolini.

* Tel.: 963544879 (E.G.-E.).

10.1021/jo061326e CCC: $33.50
Published on Web 10/26/2006

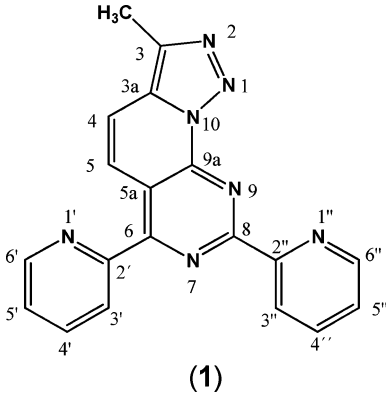

(**1**)

FIGURE 1.

a red shift in the absorption spectrum and an increase in the molar absorption coefficient. Fluorescence spectra present changes in the same direction. These photo-induced charge-transfer processes (PCT) can be advantageously used for detecting and quantifying protons and metal ions.[2−6] Most of the receptors studied up to now are based in azacrown ethers attached through nitrogen atoms to aromatic chromophores so that the connecting amino nitrogen participates in the conjugation of the aromatic moiety. In most cases, the azacrown fragment is the electron-donating part of the system while the aromatic fragment has electron-withdrawing characteristics. Coordination of the metal ion, therefore, will produce a blue shift. The number of chemosensors in which metal coordination occurs at the accepting group is, however, not so large.[1]

However, although these kinds of molecules represent the oldest type of chemosensors,[1] there is still a great interest in developing new molecules of this class, particularly for sensing biologically or environmentally relevant substrates. Anion recognition, detection, and quantification is a field of great actual upsurge, and many of the latter substrates are of anionic nature.[7−12]

Following this idea, herein we report on the triazolopyridine system 3-methyl-6,8-di(2-pyridyl)-[1,2,3]triazolo[5′,1′:6,1]pyrido[2,3-*d*]pyrimidine (**1**)[13] (Figure 1) which behaves as an interesting PCT chemosensor for metal ion and anionic species. In this report, we analyze its interaction with Cu^{2+} and Zn^{2+} metal ions, and we discuss the crystal structure of the Zn^{2+} complex $[Zn(\mathbf{1})(H_2O)_3]^{2+}$. We also show that the interaction of the Zn^{2+} complex with additional anionic and amino acid species modifies its fluorescence and UV−vis spectra allowing for their detection.

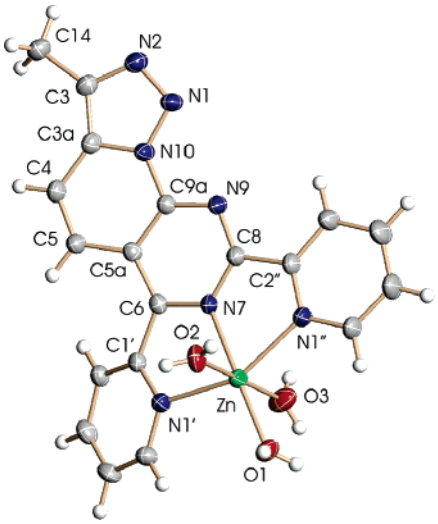

FIGURE 2. Ellipsoid plot for the cation $[Zn(1)(H_2O)_3]^{2+}$ (50% probability level). Selected bond lengths (Å) and angles (deg): Zn−O(1) 1.994(2), Zn−N(7) 2.086(2), Zn−O(3) 2.139(2), Zn−O(2) 2.139(2), Zn−N(1′) 2.141(2), Zn−N(1″) 2.163(2), O(1)−Zn−N(1′) 104.15(8), N(7)−Zn−N(1′) 75.60(8), O(1)−Zn−N(1″) 104.30(8), N(7)−Zn−N(1″) 75.84(8), N(1′)−Zn−N(1″) 151.36(8).

Results and Discussion

Crystal Structure of $[Zn(1)(H_2O)_3](ClO_4)_2]\cdot H_2O$. Crystals of $[Zn(1)(H_2O)_3](ClO_4)_2]\cdot H_2O$ were grown by slow evaporation of water−ethanol solutions containing (**1**) and $Zn(ClO_4)_2$ in equimolar amounts. Suitable crystals for X-ray analysis were obtained by recrystallization from CH_3CN solutions.

The structure consists of $[Zn(\mathbf{1})(H_2O)_3]^{2+}$ cations, perchlorate anions, and lattice water molecules. The Zn^{2+} ion is hexacoordinated by the three nitrogens of a terpyridine-like moiety (see Figure 2) with distances of Zn−N(7) = 2.086(2) Å, Zn−N(1′) = 2.141(2) Å, and Zn−N(1′′) = 2.163(2) Å and by three oxygen atoms coming from water molecules [(Zn−O(1) = 1.994(2) Å, Zn−O(2) = 2.139(2) Å, and Zn−O(3) = 2.139(2) Å)]. The coordination geometry can be defined as distorted octahedral. The terpyridine fragment imposes a meridional disposition of the ligands around the metal ion. The angles defined by the terpyridine-like moiety are shorter (Zn−N(1′)−N(7) = 75.6(8)°, Zn−N(1″)−N(7) = 75.84(8)°) than the remaining ones in agreement with the rigidity and the bite of this fragment. The dihedral angles between the pyridine moieties and the triazolopyridopyrimidine moiety, which are 26.44(7)° and 7.76(12)°, show that these units are twisted with respect to each other. One noncoordinated water molecule is hydrogen bonded to the triazol nitrogen N(2) [O(4)···N(2) = 2.822(3) Å; H(4)···N(2) = 2.069(19) Å; O(4)−H(4)···N(2) = 165(3)°]. The coordinated water molecules can be readily displaced by competitor anionic ligands (vide infra).

NMR Studies. Ligand (**1**) and its Zn^{2+} complex (**2**), which has been isolated by adding ether to a 1:1 solution of $ZnCl_2$

(1) Valeur, B. *Molecular Fluorescence. Principles and Applications;* Wiley−VCH: Weinheim, 2002.
(2) Kubo, Y.; Obara, S.; Tokita, S. *Chem. Commun*. **1999**, 2399−2400.
(3) Xiao, Y.; Fu, M.; Qian, X.; Cui, J. *Tetrahedron Lett.* **2005**, *46*, 6289−6292.
(4) Chen, C-T.; Huang, W-P. *J. Am. Chem. Soc.* **2002**, *124*, 6246−6247.
(5) Martin, M. M.; Plaza, P.; Meyer, Y. H.; Badaoui, F.; Boursom, J.; Lefèvre, J-P; Valeur, B. *J. Phys. Chem.* **1996**, *100*, 6879−6888.
(6) Callan, J. F.; de Silva, A. P.; Magri, D. C. *Tetrahedron* **2005**, *61*, 8551−8588. de Silva, A. P.; McCuaghan, B.; Mckinney, B. O.; Querol, M. *J. Chem. Soc., Dalton Trans.* **2003**, 1902−1913.
(7) Rogers, C. W.; Wolf, M. O. *Coord. Chem. Rev.* **2002**, 233−234, 341−350. Martínez-Máñez, R.; Sancenón, F. *Chem. Rev.* **2003**, *103*, 4419−4476. Snowden, T. S.; Anslyn, E. V. *Curr. Opin. Chem. Biol.* **1999**, *3* (16), 740−746.
(8) Bianchi, A.; Bowman-James, K.; García-España, E. *Supramolecular Chemistry of Anions*; Wiley−WCH: New York, 1997.
(9) Hayashita, T.; Onodera, T.; Jato, R.; Nishizawa, S.; Teramae, N. *Chem. Commun*. **2000**, 755−756.
(10) Kato, R.; Nishizawa, S.; Hayashita, T.; Teramae, N. *Tetrahedron Lett.* **2001**, *42*, 5053−5056.
(11) Jiménez, D.; Martínez-Máñez, R.; Sancenón, F.; Soto, J. *Tetrahedron Lett.* **2002**, *43*, 2823−2825.
(12) Vazquez, M.; Fabbrizzi, L.; Taglietti, A.; Pedrido, R. M.; González-Noya, A. M.; Bermejo, M. R. *Angew. Chem., Int. Ed.* **2004**, *43*, 1962−1965.
(13) Abarca, B.; Ballesteros, R.; Chadlaoui, M.; Aucejo, R.; García-España, E.; Ramírez de Arellano, C. *ARKIVOC* **2005**, *XIV*, 71−75.

TABLE 1. ^{1}H NMR δ Values of Ligand 1 and Complex 2 in DMSO

	1	2	$\Delta\delta$
H5	8.70 d $J = 9.60$ Hz	8.65 d $J = 9.60$ Hz	+0.05
H4	7.98 d $J = 9.60$ Hz	8.16 d $J = 9.60$ Hz	−0.18
H6′	8.91 dd $J_1 = 5.20$ Hz $J_2 = 1.74$ Hz	9.05 d $J = 4.00$ Hz	−0.14
H5′	7.71 ddd $J_1 = 5.20$ Hz $J_2 = 7.78$ Hz $J_3 = 1.02$ Hz	8.00−7.87 m 2H*	
H4′	8.19 ddd $J_1 = 7.92$ Hz $J_2 = 7.78$ Hz $J_3 = 1.74$ Hz	8.42−8.31 m 2H**	
H3′	8.52 dd $J_1 = 7.92$ Hz $J_2 = 1.02$ Hz	8.72 d $J = 7.24$ Hz	−0.2
H6″	8.90 dd $J_1 = 4.58$ Hz $J_2 = 1.77$ Hz	8.97 d $J = 4.26$ Hz	−0.07
H5″	7.64 ddd $J_1 = 4.58$ Hz $J_2 = 7.74$ Hz $J_3 = 1.00$ Hz	8.00−7.87 m 2H*	
H4″	8.11 ddd $J_1 = 7.97$ Hz $J_2 = 7.74$ Hz $J_3 = 1.77$ Hz	8.42−8.31 m 2H**	
H3″	8.72 dd $J_1 = 7.97$ Hz $J_2 = 1.00$ Hz	8.88 dd $J = 7.74$ Hz	−0.16
CH_3	2.65 s	2.72 s	−0.07

and (**1**) in CH_2Cl_2, have been studied by NMR in d^6-DMSO (Tables 1 and S1 in Supporting Information). All of the signals in the ^{1}H NMR have been assigned by means of COSY and total correlation spectroscopy experiments, and considering that, because of its greater deshielding relative to H3 in pyridine,[14] H3″ would be affected by two pyrimidine nitrogen lone pairs while H3′ would only be affected by one pyrimidine nitrogen lone pair. All ^{13}C NMR signals have been assigned by gradient heteronuclear single quantum correlation experiments. Although the ^{1}H NMR shifts induced by complexation are pretty small and hence a little indicative, the data of (**2**) show significant deshielding for H4, H3′, H6′, H3″, and H6″ protons, a small shielding for H5 proton, and broadening of the H4′, H4″, H5′, and H5″ signals. All ^{13}C NMR signals experience a small deshielding upon complexation, the largest one being that of C4.

The NOESY spectrum of the ligand (**1**) shows a NOE correlation peak between the H4 and the CH_3 group and more interestingly between H3′ and H3″; however, the NOESY spectrum of complex (**2**) has not shown this type of interaction between H3′ and H3″. These observations agree with a Zn^{2+} coordination through the terpyridine-like moiety formed by the two pyridine rings and the pyrimidine unit (Figure 2). Another interesting feature in the ^{1}H NMR spectrum is the smaller coupling constant values found in the complex. All these data also agree with the coordination mode observed in the crystal structure.

Spectrophotometric and Spectrofluorimetric Measurements. The electronic UV−vis spectra of (**1**) in ethanol consist of two bands centered at 290 nm ($\epsilon = 16\,500$ L mol^{-1} cm^{-1}) and 373 nm ($\epsilon = 12\,430$ L mol^{-1} cm^{-1}). Addition of Cu^{2+} produces large bathochromic shifts of the band at 373 nm which appears at 458 nm. When Zn^{2+} is added, the observed shift is less pronounced (382 nm). Nonetheless, the produced shifts are large enough to turn the initially colorless solution into yellow. These different displacements would allow this molecule to be used as a colorimetric sensor for metal ions.

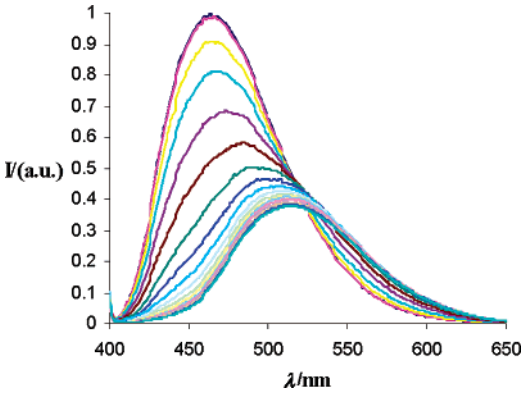

FIGURE 3. Emission spectra of ethanolic solutions containing (**1**) (1×10^{-5} M) and increasing amounts of Zn^{2+} (1×10^{-3} M) (0, 10, 100, 200, 300, 400, 500, 600, 700, 800, 900, 1000, 1100, 1200, 1300, 1400, 1500, and 1600 μL of Zn^{2+} were added).

If we now look to the emissive properties, (**1**) presents a very intense fluorescence emission at 464 nm ($\lambda_{exc} = 398$ nm). The quantum yield, Φ, of (**1**), calculated using an ethanolic solution of anthracene as reference, was 0.13. Addition of Cu^{2+} yields a strong quenching of the emission at 464 nm. The position and shape of the emission band remain constant. Addition of Zn^{2+} also provokes a quenching of the emission, although less sharp (Figure 3). However, this phenomenon is accompanied with a great bathochromic shift; the emission moves from 464 to 510 nm. This behavior resulted from a molecular fluorescent sensor operating with an internal charge-transfer mechanism.[15] Again, the different behaviors observed for Zn^{2+} and Cu^{2+} would allow for the molecule's use as a metal ion fluorimetric molecular probe.

Preliminary calculations[16] effectively show that the electron density in (**1**) accumulates in the triazol part that will act as an electron-donor group toward the electron-accepting part that resides in the 2,4-di-pyridin-2-yl-pyrimidine moiety. Moreover, compound 1-(2,4-di-(pyridin-2-yl)pyrido[2,3-*d*]pyrimidin-7-yl)-ethanone (**3**),[17] obtained by a reaction with acetic acid giving the triazolo ring opening of (**1**) with the loss of dinitrogen[18] (see Figure 4), does not show any significant emission, confirming the role of the triazolopyridine ring on the fluorescence of the system.[19]

Because of the very particular changes induced by Zn^{2+} coordination, we have checked this system for detecting anions. The idea would be to analyze the effects on the UV−vis and

(14) Hanan, G. S.; Schubert, U. S.; Volkmer, D.; Rivière, E.; Lehn, J-M.; Kyritsakas, N.; Fischer, J. *Can. J. Chem.* **1997**, *75*, 169−182.

(15) Lakowicz, J. R. *Principles of Fluorescence Spectroscopy*; Kluwer Acdamic/Plenum Publisher: New York, 1999.

(16) Stewart, J. J. P. *Rev. Comput. Chem.* **1990**, *1*, 45.

(17) 1-(2,4-Di-pyridin-2-yl-pyrido[2,3-d]pyrimidin-7-yl)-ethanone (**3**). Oily product, HRMS (EI), M^+: calcd for $C_{19}H_{13}N_5O$, 327.1120; found, 327.1127. ^{1}H NMR ($CDCl_3$): δ 9.66 (d, $J = 8.7$Hz, 1H), 8.91 (d, $J = 4.3$Hz, 1H), 8.80−8.78 (m, 2H), 8.54 (d, $J = 6.9$Hz, 1H), 8.24 (d, $J = 8.7$Hz, 1H), 7.99−7.88 (m, 2H), 7.41−7.53 (m, 2H), 2.92 (s, 3H,).

(18) Jones, G.; Mouat, D. J.; Tonkinson, D. J. *J. Chem. Soc., Perkin Trans. 1* **1985**, 2719−2723.

(19) Abarca, B.; Aucejo, R.; Ballesteros, R.; Blanco, F.; García-España, E. *Tetrahedron Lett.* **2006**, *47*, 8101−8103.

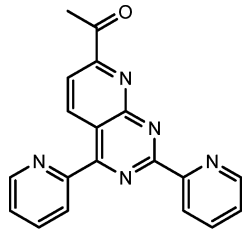

(**3**)

FIGURE 4. Structure of (**3**).

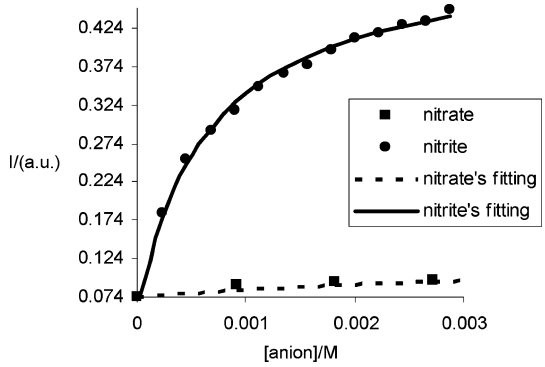

FIGURE 5. Plot of the fluorescence emission intensity versus the anion concentration including the fitting for the systems $[Zn(\mathbf{1})]^{2+}$−nitrite and $[Zn(\mathbf{1})]^{2+}$−nitrate.

fluorescence emission spectra of different anions binding to Zn^{2+}. The anions checked have been nitrate, nitrite, dihydrogenphosphate, sulfate, and chloride.

Addition of aqueous solutions of chloride, dihydrogenphosphate, sulfate, or nitrite anions to an ethanolic solution containing $Zn(ClO_4)_2 \cdot 6H_2O$ and (**1**) in a 10:1 molar ratio yields very marked hypsochromic shifts, both of the UV−vis and of the emission bands, and regains the intensity. Although these spectral features look like those of free (**1**), the ^1H NMR spectra of solutions containing Zn^{2+}:(**1**) and an excess of dihydrogenphosphate show that the binding of Zn^{2+} to the terpyridine-like unit is preserved and that demetallation processes do not occur. The changes observed in the UV−vis and emission spectra are, however, practically negligible in the case of nitrate (see Figure 5) indicating that nitrate has a much lower tendency than nitrite to coordinate to the metal. The coordination of the target anions to the Zn(II) ion should give back electron density to the terpyridine fragment restoring, to some extent, the polarity of the system.

ESI MS support the formation of 1:1 $[Zn(\mathbf{1})]^{2+}$−anion aggregates for the anions Cl^-, NO_2^-, and NO_3^-. Peaks are found, as a strong cluster of signals with a good match for the theoretical isotopic configuration, at *m*/*z* 438 to 444 for $[Zn(\mathbf{1})(Cl)]^+$, 449 to 453 for $[Zn(\mathbf{1})(NO_2)]^+$, and 465 to 469 for $[Zn(\mathbf{1})(NO_3)]^+$. In all cases, the molecular ions lose nitrogen giving (M-28) ions, as is characteristic of triazolopyridine systems, keeping the isotopic configuration.

Nonlinear regressions of the curves, like those shown in Figure 5, assuming 1:1 anion−$[Zn(\mathbf{1})]^{2+}$ stoichiometries, fit very well the experimental points and allow for the derivation of the association constants for the anions studied.[20] Figure 5 plots the emission intensity at 464 nm (λ_{exc} = 398 nm) versus anion concentration for nitrate and nitrite as a representative example.

(20) Čudić, P.; Žinić, M.; Vladislav, T.; Simeon, V.; Vigneron, J.-P.; Lehn, J.-M. *J. Chem. Soc., Chem. Commun.* **1996**, 1073−1075.

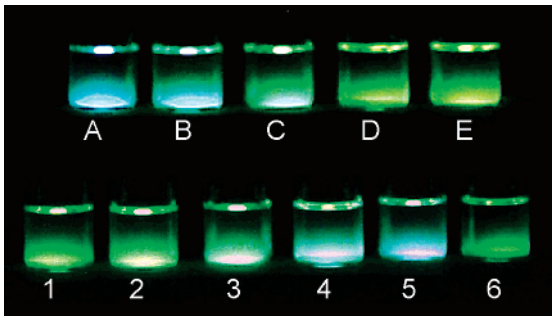

FIGURE 6. Changes in color upon irradiation with an UV of : (cuvette A) $[(\mathbf{1})] = 1.04 \times 10^{-3}$ M, (cuvette B) $[(\mathbf{1})] = 1.04 \times 10^{-3} + [Zn^{2+}] = 3.22 \times 10^{-5}$ M, (cuvette C) $[(\mathbf{1})] = 1.04 \times 10^{-3} + [Zn^{2+}] = 6.44 \times 10^{-5}$ M, (cuvette D) $[(\mathbf{1})] = 1.04 \times 10^{-3} + [Zn^{2+}] = 9.66 \times 10^{-5}$ M, (cuvette E) $[(\mathbf{1})] = 1.04 \times 10^{-3} + [Zn^{2+}] = 1.29 \times 10^{-3}$ M; (cuvette 1) $[(\mathbf{1})] = 1.04 \times 10^{-3} + [Zn^{2+}] = 1.29 \times 10^{-3}$, (cuvette 2) $[(\mathbf{1})] = 1.04 \times 10^{-3} + [Zn^{2+}] = 1.29 \times 10^{-3} + [NO_2^-] = 6.66 \times 10^{-5}$, (cuvette 3) $[(\mathbf{1})] = 1.04 \times 10^{-3} + [Zn^{2+}] = 1.29 \times 10^{-3} + [NO_2^-] = 1.33 \times 10^{-4}$, (cuvette 4) $[(\mathbf{1})] = 1.04 \times 10^{-3} + [Zn^{2+}] = 1.29 \times 10^{-3} + [NO_2^-] = 2 \times 10^{-4}$, (cuvette 5) $[(\mathbf{1})] = 1.04 \times 10^{-3} + [Zn^{2+}] = 1.29 \times 10^{-3} + [NO_2^-] = 3.33 \times 10^{-4}$, (cuvette 6) $[(\mathbf{1})] = 1.04 \times 10^{-3} + [Zn^{2+}] = 1.29 \times 10^{-3} + [NO_3^-] = 3.33 \times 10^{-4}$.

The values obtained (K_a (NO_2^-) = 1.5×10^3 M^{-1}, K_a (SO_4^{2-}) = 2.5×10^3 M^{-1}, K_a ($H_2PO_4^-$) = 4.8×10^4 M^{-1}, K_a (Cl^-) = 3.20×10^3 M^{-1}) show that dihydrogenphosphate presents one order of magnitude higher affinity for (**1**) than any one of the other anions. For nitrate, it was not even possible to calculate a stability constant value because of its very low interaction.

Therefore, this system will permit the direct detection of anions without the need of using competitive reactions or dyes. One of the most interesting aspects is the discrimination between nitrite and nitrate anions. In Figure 6 , the changes in color experienced by solutions of (**1**) when adding increasing amounts of Zn^{2+}, nitrite, and nitrate and upon excitation with an UV lamp are presented.

Ligand (**1**) presents an emission band in the blue region (cuvette A in Figure 6) which is shifted to the green region (cuvette E in Figure 6) upon addition of Zn^{2+} solutions. While addition of nitrite leads to a recovery of the blue emission (cuvette 5 in Figure 6), addition of the same amount of nitrate does not yield any significant change (cuvette 6 in Figure 6). Experiments performed in the presence of both anions confirmed the expected selectivity. The ability of the Zn^{2+} complex to interact and quantify amino acids has been explored for L-glutamate and L-aspartate.[21−25] Addition of the amino acids produces a fluorescent response similar to that with the addition of the anions, namely, a hypsochromic shift and recovery of the emission intensity (Figure 7). The stability constants calculated for the aminoacids are as follows; K_a (L-aspartic) = 1×10^4, K_a (L-glutamic) = 5.5×10^3.

Actually, we are exploring the effects of replacing the methyl group at the 3-position by other electron-withdrawing or electron-donating groups on the electronic and emission proper-

(21) Fabbrizzi, L.; Licchelli, M.; Perotti, A.; Poggi, A.; Rabaioli, G.; Sacchi, D.; Taglietti, A. *J. Chem. Soc., Perkin Trans. 2* **2001**, 2108−2113.
(22) Folmer-Andersen, J. F.; Lynch, V. M.; Anslyn, E. V. *Eur. J. Chem.* **2005**, *11* (18), 5319−5326.
(23) Folmer-Andersen, J. F.; Lynch, V. M.; Anslyn, E. V. *J. Am. Chem. Soc.* **2005**, *127* (22), 7986−7987.
(24) Nguyen, B. T.; Wiskur, S. L.; Anslyn, E. V. *Org. Lett.* **2004**, *6* (15), 2499−2501.
(25) Ait-Haddou, H.; Wiskur, S. L.; Lynch, V. M.; Anslyn, E. V. *J. Am. Chem. Soc.* **2001**, *123* (45), 11296−11297.

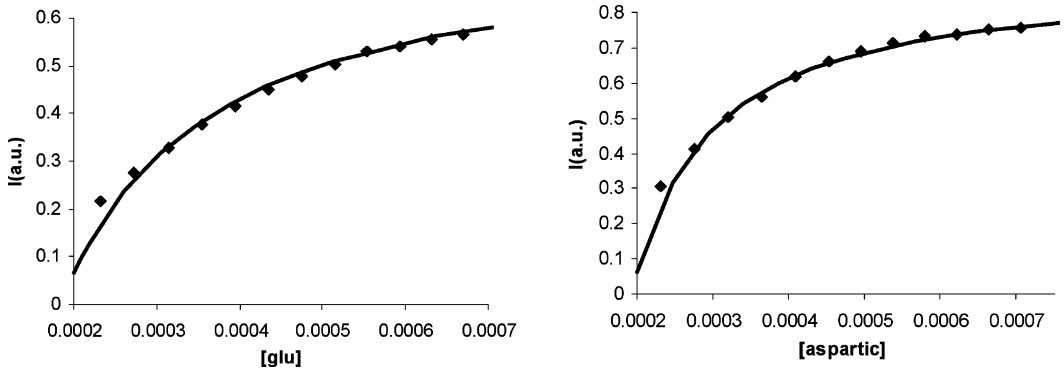

FIGURE 7. Plot of the fluorescence emission intensity versus the anion concentration including the fitting for the systems: left, $[Zn(\mathbf{1})]^{2+}$−L-glutamate and $[Zn(\mathbf{1})]^{2+}$−L-aspartate.

ties of the systems, and we are checking the possibility of our system as an alternative method for the detection of anions, in particular, the nitrite anion.

Experimental Section

Synthesis of (1). Ligand (**1**) has been synthesized as described in ref 26 by the reaction of 7-lithio-3-methyl-[1,2,3]triazolo[1,5-*a*]pyridine with 2-cyanopyridine and has been identified by X-ray diffraction analysis.[13]

Synthesis of $[Zn(1)(H_2O)_3](ClO_4)_2]\cdot H_2O$. A total of 0.031 g (0.1 mmol) of (**1**) was dissolved in the minimum amount of ethanol, and then 0.037 g (0.1 mmol) of $ZnClO_4\cdot 6H_2O$ was added to the solution obtaining a bright yellow solution. After a few days, crystals from $[Zn(\mathbf{1})(H_2O)_3](ClO_4)_2]\cdot H_2O$ appeared, then they were filtered and recrystallized in MeCN. Anal. Calcd for $C_{18}H_{21}N_7ZnO_{12}Cl_2$: C, 33.2; H, 3.4; N, 12.9. Found: C, 33.5; H, 3.2; N, 13.0.

Materials and Methods

NMR Measurements. The ^1H and ^{13}C NMR spectra were recorded on a 300 MHz spectrometer operating at 299.95 MHz for ^1H and at 75.43 MHz for ^{13}C. For the ^{13}C NMR spectra, dioxane was used as a reference standard ($\delta = 67.4$), and for the ^1H NMR spectra, the solvent signal was used.

Spectrophotometric and Spectrofluorimetric Titrations. The absorbance of the excitation wavelength was maintained lower than 0.15. When excitation was carried out at wavelengths different than the isobestic points, a correction for the absorbed light was performed.

The 10^{-5} M solutions of (**1**) were prepared using dry ethanol as a solvent. Cu^{2+} and Zn^{2+} solutions were prepared solving the correspondent perchlorate in Millipore water in a 10^{-3} mol dm^{-3} concentration. Work solutions were obtained mixing 10 mL of the solution of (**1**) with the corresponding amounts of the solutions of the metals. The 10^{-3} mol dm^{-3} aqueous solutions of the anions were prepared from Na_2SO_4, NaCl, KH_2PO_4, $NaNO_2$, and $NaNO_3$ analytical grade salts. The 10^{-3} M L-glutamic and L-aspartic solutions were prepared from analytical grade samples.

Acknowledgment. Financial support from DGICYT Project No. BQU2003-09215-CO3 and No. BQU2003-09215-CO1 is gratefully acknowledged. R.A. wants to thank Ministerio de Educación, Cultura y Deporte for a predoctoral fellowship.

Supporting Information Available: Job plot for the system Cu^{II}−(**1**); plot of the fluorescence emission intensity versus the phosphate concentration and the fitting curve; plot of the fluorescence emission intensity versus the sulfate concentration and the fitting curve; plot of the fluorescence emission intensity versus the chloride concentration and the fitting curve; ^{13}C NMR data for (**1**) and (**2**); and crystallographic data for $[Zn(\mathbf{1})(H_2O)_3](ClO_4)_2]\cdot H_2O$ in CIF format. This material is available free of charge via the Internet at http://pubs.acs.org.

JO061326E

(26) Abarca, B.; Ballesteros, R.; Chadlaoui, M. *ARKIVOC* **2002**, *X*, 52−60.